



## The geometry and absorption of diketo-pyrrolo-pyrroles substituted with various aryls

Stanislav Luňák Jr.<sup>a</sup>, Lukáš Havel<sup>a</sup>, Jan Vyňuchal<sup>b,c,\*</sup>, Petra Horáková<sup>a</sup>, Jiří Kučerík<sup>d</sup>, Martin Weiter<sup>d</sup>, Radim Hrdina<sup>a</sup>

<sup>a</sup> Department of Organic Technology, Faculty of Chemical Technology, University of Pardubice, Studentská 95, CZ-532 10 Pardubice, Czech Republic

<sup>b</sup> Research Institute of Organic Syntheses, Rybitví 296, CZ-533 54 Rybitví, Czech Republic

<sup>c</sup> Synthesia a.s., Pardubice, Semtín 103, CZ-532 17 Pardubice, Czech Republic

<sup>d</sup> Faculty of Chemistry, Brno University of Technology, Purkyňova 118, CZ-612 00 Brno, Czech Republic

### ARTICLE INFO

#### Article history:

Received 30 June 2009

Received in revised form

25 September 2009

Accepted 28 September 2009

Available online 1 October 2009

#### Keywords:

Diketo-pyrrolo-pyrroles (DPP)

Time dependent density functional theory

(TD DFT)

Absorption

Fluorescence

### ABSTRACT

A series of five symmetrical and four unsymmetrical diaryl substituted diketo-pyrrolo-pyrroles was synthesized; two unsymmetrical derivatives are reported for the first time. The relationship between the theoretical excitation energies of the  $S_0 \rightarrow S_1$  transition, computed by time dependent density functional theory and the experimental positions of 0–0 vibronic bands in the visible absorption (or fluorescence excitation) spectra was studied. Experimental data were obtained from either solution or from low temperature organic solvent glass, in which the progressions of the vibrational structure enabled correct assignment of vibronic sub-bands in some cases. Theoretical calculations predicted that a linear bathochromic and hyperchromic shift would accompany substitution of each phenyl in the parent 3,6-diphenyl-2,5-dihydro-pyrrolo[3,4-c]pyrrole-1,4-dione by providing a more extensively conjugated aryl centre (2-naphthyl, biphenyl, stilbenyl) for the ensuing planar derivatives. Qualitatively, the experimental bathochromic shifts of the 0–0 vibronic sub-bands were in exact agreement with theory, whilst hyperchromic shifts were affected by the very low solubility of the planar, symmetrical derivatives. Deviations from this ideal behaviour were observed for non-planar derivatives (aryl = stilbenyl or 1-naphthyl), for which the dihedral angles describing the aryl, out-of-plane torsions were probably underestimated by DFT.

© 2009 Elsevier Ltd. All rights reserved.

### 1. Introduction

The present authors have recently shown that calculations based on time dependent density functional theory (TD DFT) could predict the absorption maxima of diketo-pyrrolo-pyrrole (DPP) pigments which had been substituted with various combinations of strong electron-donating and electron-withdrawing substituents in the *para* positions of both pendant phenyl rings [1]. A necessary component of such computation was the introduction of solvent effects by a polarized continuum model (PCM). The aim of this paper is to challenge this methodology by interpreting the relationship between structure and absorption of a series of symmetrical and unsymmetrical DPPs that comprise different combinations of aryl substituents (Table 1).

3,6-Diphenyl-2,5-dihydro-pyrrolo[3,4-c]pyrrole-1,4-dione (**BPPB** in our notation) is a basic chromophore of this set; it has been patented by CIBA [2]. **BPPB** itself (C.I. Pigment Red 255) and at least

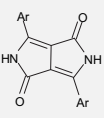
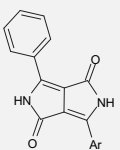
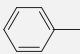
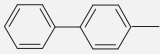

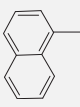
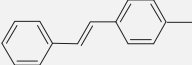
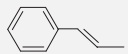
five its symmetrical derivatives substituted on phenyl form a commercially very successful family of high performance organic pigments [3]. One of them, **BiPPBi** (C.I. Pigment Red 264) was also used in this study. These two pigments are the only ones from the model set, for which the structure was estimated experimentally using X-ray diffraction [4,5]. The other compounds under study were not commercialised at the time of manuscript preparation.

Extensive literature exists on DPPs in general and, more specifically, in relation to commercial examples; in this context, >279 references exist for **BPPB** and 138 for **BiPPBi** were found as at 08/06/2009. In contrast, there is a paucity of citations relating to other symmetrical derivatives, with just 6 references to **1NPP1N**, 7 for **2NPP2N** and 2 for **StPPSt** being found in patent literature. Four patents discuss the asymmetrical compound **BiPPB** and 1 patent describes **1NPPB**; as no references relating to the 2-naphthyl compound **2NPPB** and the stilbene analogue **StPPB** were found, the syntheses of these two particular compounds was described in detail. Styryl (phenyl-ethenyl) **PePPB** and **PePPPe** derivatives were handled only theoretically, as a synthetic route to these compounds is not known [6].

With exception of the authors' previous work [1], no *ab initio* calculations of DPP pigments have been published and references

\* Corresponding author at: Research Institute of Organic Syntheses, Rybitví 296, CZ-533 54 Rybitví, Czech Republic. Tel.: +420 466 823 351; fax: +420 466 822971. E-mail address: [jan.vynuchal@vuos.com](mailto:jan.vynuchal@vuos.com) (J. Vyňuchal).

**Table 1**  
Notation of the compounds studied.

| Ar  | <br>symmetrical |              | <br>unsymmetrical |
|---|--|--------------|--|
|    | <b>BPPB</b>  | –            |  |
|    | <b>BiPPBi</b>  | <b>BiPPB</b> |  |
|    | <b>2NPP2N</b>  | <b>2NPPB</b> |  |
|    | <b>1NPP1N</b>  | <b>1NPPB</b> |  |
|    | <b>StPPSt</b>  | <b>StPPB</b> |  |
|  | <b>PePPPe</b>  | <b>PePPB</b> |  |

to only semiempirical PPP [7] and INDO/S studies on **BPPB** and its aggregates [8] were found. The latter computations were based on X-ray geometry [7] which was later revised [4] and which underestimated the visible absorption maximum compared to its experimental counterpart [9].

## 2. Experimental

### 2.1. Syntheses and analysis

**BPPB** was synthesized from benzonitrile and diisopropyl succinate [10]. Other symmetrical derivatives (**BiPPBi**, **1NPP1N**, **2NPP2N** and **StPPSt**) were synthesized in an analogous manner from corresponding nitriles purchased from Aldrich, except for 4-cyano-stilbene, which was synthesized as described below. The purity of all compounds was determined using elemental analysis, MS and  $^1\text{H}$  NMR.

The unsymmetrical derivatives (**BiPPB**, **1NPPB** and **StPPB**) were synthesized by the base-catalysed condensation of ethyl 4,5-dihydro-5-oxo-2-phenyl(1H)pyrrole-3-carboxylate (phenyl-pyrrolinone ester) as described previously [11] with the above mentioned nitriles. **2NPPB** was synthesized from benzonitrile and ethyl 4,5-dihydro-5-oxo-2-(2-naphthyl)-(1H)pyrrole-3-carboxylate (2-naphthyl-pyrrolinone ester), which synthesis is described below. The syntheses of two till unknown unsymmetrical derivatives (**2NPPB** and **StPPB**) is presented in detail.

#### 2.1.1. Syntheses of 4-cyano-stilbene

Triethanolamine (200 ml), 4-bromobenzonitrile (18.2 g, 0.1 mol), styrene (10.4 g, 0.1 mol) and palladium acetate (0.23 g, 1 mmol) were

charged into a 0.5 l Keller flask equipped with a stirrer, reflux condenser, thermometer and a nitrogen inlet. The reaction mixture was heated out at 100 °C for 10 h. After a cooling to room temperature the product was extracted with ether (2 × 300 ml). The ether layers were washed with water, dried with magnesium sulphate and evaporated. The yellow product was dissolved by stirring in methanol (which removed triethanolamine), filtered and dried. Yield: 19.47 g (95%). The melting point was 116–118 °C (lit. [12] 117–119 °C).

#### 2.1.2. Syntheses of ethyl 4,5-dihydro-5-oxo-2-(2-naphthyl)-(1H)pyrrole-3-carboxylate (2-naphthyl-pyrrolinone ester)

**2.1.2.1. Preparation of ethyl 2-naphthoate.** 2-Naphthoic acid (Aldrich, 60 g, 0.348 mol), ethanol (226 ml) and sulphuric acid (7 ml) were added to the two-necked flask equipped with thermometer, stirrer and refluxing condenser. The reaction mixture was heated to reflux for 10 h and after that the mixture was cooled to room temperature; excess ethanol was distilled off. The ensuing product was extracted with diethyl ether; the organic layer was separated, washed with sodium carbonate (5%) and water and then dried over  $\text{Na}_2\text{SO}_4$ . The solvent was removed under reduced pressure. The amount of the oily product was 52 g (yield 75%).

**2.1.2.2. Preparation of ethyl 3-(2-naphthyl)-3-oxopropanoate.** A mixture of sodium hydride (caution: reacts violently with water, liberating hydrogen; incompatible with water, acids, alcohols, strong oxidizing agents; Aldrich 60%, 16.8 g, 0.42 mol), ethyl 2-naphthoate obtained by Section 2.1.2.1 (42 g, 0.21 mol) and 1-butoxybutane (360 ml) was added to the three neck flask equipped with thermometer, stirrer, dropping funnel and refluxing condenser. The reaction mixture was heated to 100 °C and ethyl acetate (27.6 g, 0.313 mol) in 1-butoxybutane (20 g) was added to the mixture by means of dropping funnel within about 1.5 h. The suspension was heated to reflux for 6 h, then cooled to room temperature and diluted with diethyl ether (100 ml). The obtained salt was filtrated off, washed with diethyl ether (300 ml). Subsequently, the suspension was poured onto 300 g ice and acidified by hydrochloric acid to pH = 2. The product was extracted with diethyl ether, organic layer was separated, washed with sodium carbonate (5%) and water. Then dried over  $\text{Na}_2\text{SO}_4$ . The solvent was removed under reduced pressure. The amount of oily product was 32.4 g (64% of theory).

**2.1.2.3. Preparation of ethyl 4,5-dihydro-5-oxo-2-(2-naphthyl)-(1H)pyrrole-3-carboxylate.** Ethyl 3-(2-naphthyl)-3-oxopropanoate (32.4 g, 0.134 mol) obtained by Section 2.1.2.2, ethyl bromoacetate (24.6 g, 0.147 mol), sodium carbonate (19.3 g), acetone (32 ml) and ethyleneglycol dimethylether (32 ml) were added to the three-necked flask equipped with thermometer, stirrer and refluxing condenser. The reaction mixture was refluxed for 14 h. Acetone was continuously added into the reaction mixture to keep the constant volume due to evaporating off. Subsequently, the mixture was cooled down at room temperature and inorganic salt was filtrated and washed by acetone. The filtrate and acetone from the washing process was combined and acetone was distilled off with other volatile fractions up to 150 °C under nitrogen. Acetic acid (101 ml) and ammonium acetate (58 g) were added to the dark liquid distilling residue. The mixture was kept under reflux at 120 °C for 4 h. 16.1 g (yield 43%) of a product was obtained by filtration from the mixture after the cooling. A sample for analysis was recrystallized from toluene. The melting point was 188–193 °C.

Calculated: C (72.58), H (5.37), N (4.98). Found: C (72.50), H (5.35), N (5.11).

MW = 281 Da; positive-ion APCI-MS:  $m/z$  282  $[\text{M} + \text{H}]^+$  (100%)  $^1\text{H}$  chemical shifts: 10.83 (1H, s, NH); 8.21–7.61 (7H, m, ArH); 4.05 (2H, q,  $\text{CH}_2$ ); 3.49 (2H, s,  $\text{CH}_2$ ); 1.10 (3H, t,  $\text{CH}_3$ ).

### 2.1.3. Syntheses of 3-(2-naphthyl)-6-phenyl-2,5-dihydropyrrolo[3,4-c]pyrrole-1,4-dione (2NPPB)

*tert*-Amyl alcohol (33 ml) and sodium metal (caution: reacts violently with water, liberating hydrogen; flammable solid; incompatible with water, strong oxidizing agents; air sensitive; 0.7 g, 30 mmol) were charged into a 100 ml three-necked flask equipped with a stirrer, reflux condenser and thermometer. The sodium metal was dissolved under reflux in the presence of catalytic amount of FeCl<sub>3</sub> (which approximately took 1 h), whereupon benzonitrile (1.4 g, 13.6 mmol) was added. 2-Naphthyl-pyrrolinone ester (2.5 g, 8.9 mmol), obtained according to Section 2.1.2.3 was continuously introduced in small amounts over 0.5 h. The ensuing mixture was stirred under reflux for 1 h and the hot suspension was then filtered, the filter cake suspended in 100 ml *tert*-amyl alcohol and then 10 ml acetic acid was added to protolyse the salt. Protolysis was carried out at 100 °C for 2 h. The resulting hot suspension was filtered, and the filter cake was washed with hot water to neutral washings. The filter cake was suspended in 300 ml methanol. The suspension was heated to boiling and refluxed for 2 h. The hot suspension was filtered, washed with ethanol and hot water. Yield: 1.5 g (54%).

Calculated: C(78.09), H(4.17), N(8.28). Found C(77.19), H(4.20), N(8.06)

MW = 338 Da; Negative-ion APCI-MS:  $m/z$  337 [M – H]<sup>–</sup> (100%)

<sup>1</sup>H chemical shifts: 11.45 (2H, br s, NH); 9.03 (1H, m); 8.7 (1H, m); 8.55(2H, m); 8.14(1H, m); 8.04 (1H, m); 8.00 (1H, m); 7.56–7.72 (5H, m).

<sup>13</sup>C chemical shifts were not determined due to a very low solubility of the sample.

### 2.1.4. Syntheses of 3-(4-stilbenyl)-6-phenyl-2,5-dihydropyrrolo[3,4-c]pyrrole-1,4-dione (StPPB)

*tert*-Amyl alcohol (67 ml), sodium metal (1.43 g, 97 mmol) and a catalytic amount of FeCl<sub>3</sub> were charged into a 250 ml three-necked flask equipped with a stirrer, reflux condenser, thermometer and nitrogen inlet. The sodium metal was dissolved under the reflux, whereupon 4-cyano-stilbene (6.4 g, 31 mmol) obtained according to Section 2.1.1 was added. After that phenyl-pyrrolinone ester (7.27 g, 31 mmol) was added within 0.5 h. Finally, this mixture was stirred and refluxed for 2 h. The reaction mixture was cooled to a 60 °C and infused into 200 ml distilled water. The mixture was carried out at 80 °C for 2 h. The resulting hot suspension was filtered and filter cake was washed with 35 ml of hot isopropyl alcohol and than with hot water to neutral washings. The filter cake was suspended into methanol. The suspension was heated to boiling and refluxed 0.5 h. The hot suspension was filtered, washed with methanol and dried. Yield: 6.66 g (54%).

Calculated: C(79.98), H(4.65), N(7.17). Found C(79.61), H(4.62), N(7.07)

MW = 390 Da; Positive-ion APCI-MS:  $m/z$  391 [M + H]<sup>+</sup> (100%)

<sup>1</sup>H chemical shifts: 11.37 (2H, br s, NH); (7.54 (1H, d,  $J$  = 16.7 Hz); 7.38 (1H, d,  $J$  = 16.7 Hz); 8.53 (4H, m); 7.86 (2H, d), 7.63 (3H, m) signals of Ar–CH = CH–Ar; 7.70 (2H, ortho, ArH); 7.47 (2H, meta, ArH), 7.38 (1H, para, ArH)

<sup>13</sup>C chemical shifts were not determined due to a very low solubility of the sample.

## 2.2. Instrumental equipment

The room temperature (DMSO) absorption measurements were carried out on a Perkin–Elmer Lambda 9 absorption spectrometer. The room temperature (DMSO, MTHF) and low temperature (MTHF,

77 K) fluorescence emission and excitation spectra were measured on Perkin Elmer LS 35 fluorescence spectrometer equipped with commercial low temperature accessory.

Thermogravimetric studies (TGA) were performed using TA Instruments TGA Q5000 (New Castle, Delaware, USA) device in 100 µl open platinum pans. The samples, typically 5 mg, were heated by thermal ramp of 10 °C min<sup>–1</sup> from 40 °C to 650 °C in dynamic nitrogen atmosphere (25 ml min<sup>–1</sup>). Calorimetric analyses (DSC) were carried out employing TA Instruments DSC Q200 calorimeter equipped with external cooler RCS90 allowing experimental temperature range from –90 to 500 °C. Experiments were conducted in open TA Tzero™ aluminum pans. Thermal history of all samples was set up to be the same using of heating ramp of 3 °C min<sup>–1</sup> from 40 °C to –90 °C and then 10 °C/min<sup>–1</sup> to the temperature determined by TGA as  $T_s$  (Table 2). All DSC experiments were made under 50 ml min<sup>–1</sup> nitrogen purge. Before analyses device was calibrated for temperature and enthalpy using indium, tin and zinc standards (Perkin Elmer, Waltham, Massachusetts, USA). All the records were assessed by TA Universal Analysis 2000 software version 4.4A.

The equipment for other analytical measurements and the analytical procedures are the same as described in Ref. [1].

## 2.3. Computational procedures

The geometry of all eleven compounds was optimized using quantum chemical calculations based on DFT. Hybrid three-parameter B3LYP functional [13] in combination with 6-311G(d,p) basis was used. No constraints were preliminary employed, but, if the non-constrained computations converged to symmetrical structures, the final computations were carried out with these symmetry constraints. No imaginary frequencies were found after diagonalization of Hessian matrix, confirming that the computed geometries were real minima on the ground state hypersurfaces.

The TD DFT method was used for a computation of vertical excitation energies on the computed geometry. The same exchange-correlation functional (B3LYP) was used with rather broader basis set (6-311 + G(2d,p)) particularly efficient for TD modeling of organic dyes [14]. Solvent effect of dimethylsulfoxide (DMSO) was involved by non-equilibrium PCM [15].

All the methods were taken from Gaussian03W program suite [16], and the default values of computational parameters were used. The results were analyzed using GaussViewW from Gaussian Inc., too.

**Table 2**

Experimental absorption and fluorescence excitation and emission maxima and sublimation temperatures  $T_s$  determined by TGA.

| Comp.         | Absorption             |                         | Fluorescence          |                       |                       | $T_s$ [°C] |
|---------------|------------------------|-------------------------|-----------------------|-----------------------|-----------------------|------------|
|               | DMSO (20 °C)           |                         | MTHF (77 K)           |                       |                       |            |
|               | $\lambda_{\text{abs}}$ | $\epsilon_{\text{max}}$ | $\lambda_{\text{em}}$ | $\lambda_{\text{ex}}$ | $\lambda_{\text{em}}$ |            |
| <b>BPPB</b>   | 505                    | 34200                   | 517                   | 512                   | 515                   | 383        |
| <b>2NPP2N</b> | 529                    | 30400                   | 547                   | –                     | –                     | 463        |
| <b>2NPPB</b>  | 517                    | 37200                   | 534                   | 523                   | 527                   | 372        |
| <b>1NPP1N</b> | 471                    | 7900                    | 567                   | 498                   | 527                   | 278        |
| <b>1NPPB</b>  | 493                    | 21500                   | 558                   | 503                   | 511                   | 347        |
| <b>BiPPBi</b> | 535                    | 17300                   | 549                   | –                     | –                     | 477        |
| <b>BiPPB</b>  | 520                    | 40100                   | 535                   | 526                   | 531                   | 415        |
| <b>StPPSt</b> | 565                    | 33600                   | 578                   | –                     | –                     | 410        |
| <b>StPPB</b>  | 535                    | 44300                   | 554                   | 548                   | 550                   | 428        |

$\lambda_{abs}$ , absorption maximum [nm];  $\lambda_{ex}$ , excitation maximum [nm];  $\lambda_{em}$ , emission maximum [nm];  $\epsilon_{max}$ , molar absorptivity [l mol<sup>–1</sup> cm<sup>–1</sup>], values in italics come from insufficiently soluble compounds.

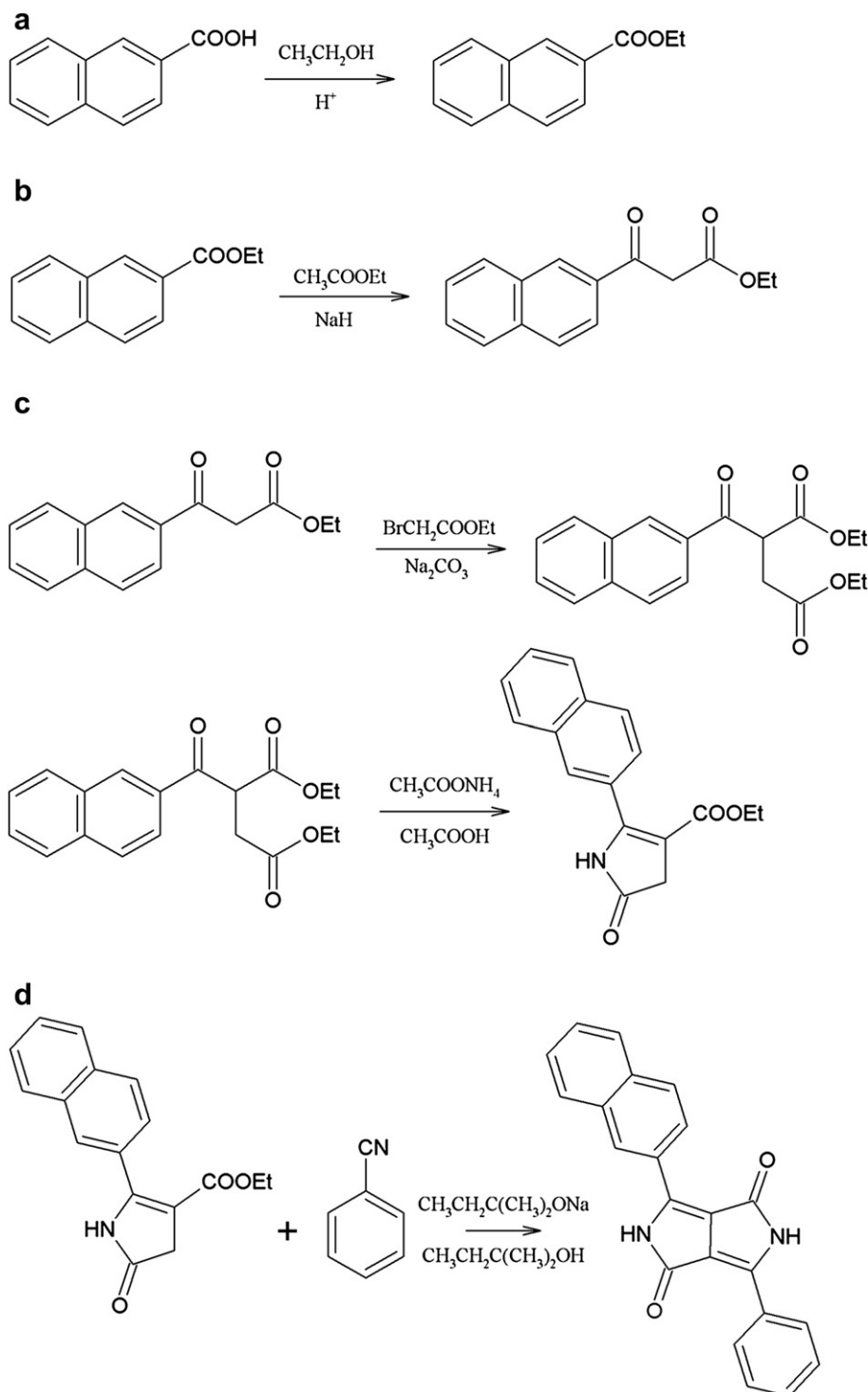
### 3. Results and discussion

#### 3.1. Syntheses and sublimation

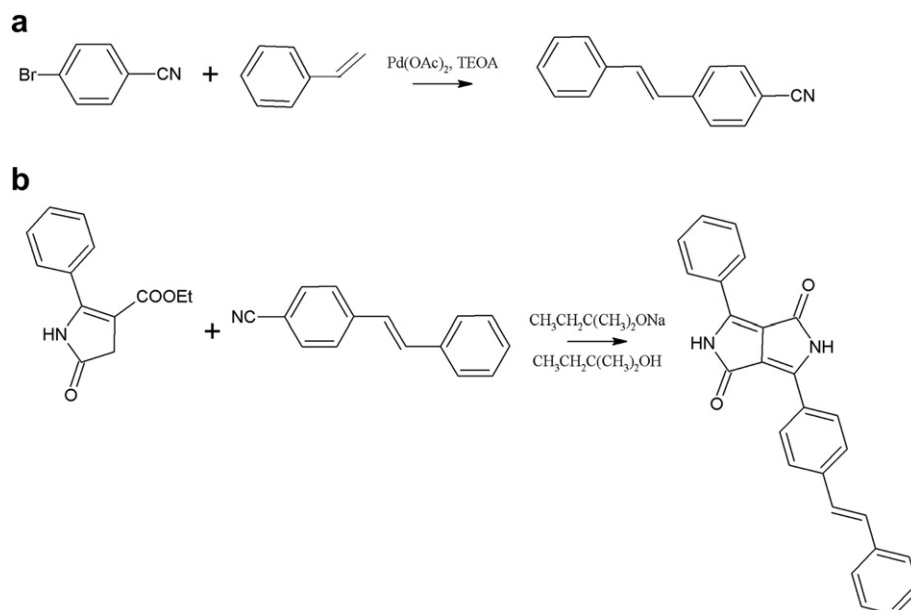
The symmetrical derivatives were synthesized from diisopropyl succinate and corresponding aromatic nitrile. The synthesis of unsymmetrical derivatives was carried out from ethyl 4,5-dihydro-5-oxo-2-phenyl(1*H*)pyrrole-3-carboxylate (phenyl-pyrrolinone ester) and corresponding aromatic nitrile (Scheme 1 for **BiPPB**),

except **2NPPB**, which was synthesized from ethyl 4,5-dihydro-5-oxo-2-(2-naphthyl)-(1*H*)pyrrole-3-carboxylate (2-naphthyl-pyrrolinone ester) and benzonitrile (Scheme 2). The reaction yields were usually over 50%. The purity of the compounds was checked by elemental analysis,  $^1\text{H}$  NMR and mass spectroscopy. For details of the syntheses and analytics see [Experimental](#).

Synthesized compounds were characterized by sublimation temperature  $T_s$  (Table 2) determined by thermogravimetry (TGA). In fact, the temperature  $T_s$  stands for the temperature at which



Scheme 1.



Scheme 2.

mass loss starts; kinetics of sublimation is very slow and thus progressive increase in temperature causes later the degradation of the sample. The char which could be seen at the end of the TGA experiment typically reached from 10 to 40% of original sample mass. Experiments carried out using differential scanning calorimetry (DSC) revealed no phase transitions within  $-90\text{ }^{\circ}\text{C}$  and  $T_s$ . TGA of **StPPB** and especially **StPPSt** show the slowest kinetics of a sublimation process, for which  $T_s$  was determined only tentatively (Table 2).

The synthesized compounds are pigments highly insoluble in common solvents, except **1NPPB** and especially **1NPP1N**. The unsymmetrical pigments (**BiPPB**, **2NPPB** and **StPPB**) are slightly better soluble than the corresponding symmetrical ones (**BiPPBi**, **2NPP2N** and **StPPSt**).

### 3.2. DFT ground state geometry and energy

The restricted B3LYP calculations resulted in a strictly planar geometry for **BPPB** and thus  $C_{2h}$  symmetry [1]. The dihedral angle between phenyl and pyrrolinone rings in unsymmetrical biphenyl substituted compound **BiPPB** was also near to zero, while between both phenyls it was about  $38^{\circ}$ . The same angle between phenyls in biphenyl moiety was found for both rotamers ( $C_2$ ,  $C_i$ ) of **BiPPBi**, which differ by a mutual orientation of rotated terminal phenyl rings. The ground state energy of  $C_i$  rotamer is negligibly higher (Table 3).

Two (three) minima of energy were found for **2NPPB** (**2NPP2N**), all of them corresponding to planar geometry (Fig. 1). The most stable rotamers are **2NPP2N** (180–180) and **2NPPB** (0–180), but the energy differences are marginal (Table 3) as the steric interaction in all two (three) rotamers is almost the same.

The situation for 1-naphthyl substituted DPPs is different. They are non-planar, as both 1-naphthyl and phenyl are always rotated out from a plane of central heterocycle. Such rotation of phenyl ring of **1NPPB**, induced by the rotation of 1-naphthyl bonded to the opposite ring of a central heterocycle, is analogous to the case of N-monoalkylated **BPPB** [10]. If planar, there should exist two (three) minima for **1NPPB** (**1NPP1N**) by analogy with 2-naphthyl conformers, differing in this case by a steric interaction of a naphthalene ring

Table 3

DFT computed relative ground state energy and PCM TD DFT computed excitation energies (converted to  $\lambda_{\text{max}}$  [nm]) and oscillator strengths ( $f_{\text{osc}}$ ) in DMSO.

| Compound      | Symmetry | Dihedral angles <sup>a</sup> | Relative internal energy <sup>b</sup> | S <sub>0</sub> → S <sub>1</sub> transition characteristics |                  |
|---------------|----------|------------------------------|---------------------------------------|--|------------------|
|               |          |                              |                                       | $\lambda_{\text{max}}$                                     | $f_{\text{osc}}$ |
| <b>BPPB</b>   | $C_{2h}$ | <b>0–0</b>                   | –                                     | 494  | 0.641            |
| <b>2NPP2N</b> | $C_{2h}$ | <b>0–0</b>                   | 0.21                                  | 523  | 1.156            |
|               | $C_s$    | <b>0–180</b>                 | 0.15                                  | 534  | 0.952            |
|               | $C_{2h}$ | <b>180–180</b>               | <b>0.00</b>                           | 542  | 0.840            |
| <b>2NPPB</b>  | $C_s$    | <b>0–0</b>                   | 0.09                                  | 509  | 0.886            |
|               | $C_s$    | <b>0–180</b>                 | <b>0.00</b>                           | 519  | 0.718            |
| <b>1NPP1N</b> | $C_i$    | <b>134–134</b>               | 12.85                                 | 493  | 0.584            |
|               | $C_2$    | <b>136–136</b>               | 12.12                                 | 497  | 0.599            |
|               | $C_i$    | <b>28–135</b>                | 11.46                                 | 516  | 0.666            |
|               | $C_i$    | <b>29–136</b>                | 10.95                                 | 513  | 0.679            |
|               | $C_i$    | <b>29–29</b>                 | 10.29                                 | 537  | 0.755            |
|               | $C_2$    | <b>29–29</b>                 | 9.64                                  | 532  | 0.767            |
| <b>1NPPB</b>  | $C_i$    | <b>7–136</b>                 | 6.19                                  | 495  | 0.611            |
|               | $C_i$    | <b>7–29</b>                  | 4.87                                  | 515  | 0.703            |
| <b>BiPPBi</b> | $C_i$    | <b>0–0</b>                   | 0.01                                  | 531  | 1.168            |
|               | $C_2$    | <b>0–0</b>                   | <b>0.00</b>                           | 531  | 1.170            |
| <b>BiPPB</b>  | $C_i$    | <b>0–0</b>                   | –                                     | 513  | 0.894            |
| <b>StPPSt</b> | $C_{2h}$ | <b>0–0</b>                   | 0.15                                  | 600  | 2.012            |
|               | $C_s$    | <b>0–180</b>                 | 0.12                                  | 601  | 1.959            |
|               | $C_{2h}$ | <b>180–180</b>               | <b>0.00</b>                           | 601  | 1.923            |
| <b>StPPB</b>  | $C_s$    | <b>0–0</b>                   | 0.06                                  | 550  | 1.355            |
|               | $C_s$    | <b>0–180</b>                 | <b>0.00</b>                           | 550  | 1.296            |
| <b>PePPPe</b> | $C_{2h}$ | <b>0–0</b>                   | 1.89                                  | 574  | 1.402            |
|               | $C_s$    | <b>0–180</b>                 | 0.89                                  | 588  | 1.128            |
|               | $C_{2h}$ | <b>180–180</b>               | <b>0.00</b>                           | 598  | 0.974            |
| <b>PePPB</b>  | $C_s$    | <b>0–0</b>                   | 0.90                                  | 534  | 1.016            |
|               | $C_s$    | <b>0–180</b>                 | <b>0.00</b>                           | 547  | 0.789            |

<sup>a</sup> The first value is the dihedral angle between phenyl and pyrrolinone, the second is between non-phenyl aryl and pyrrolinone for unsymmetrical derivatives.

<sup>b</sup> Relative to the bolded energy of most stable isomer [kcal. mol<sup>−1</sup>].



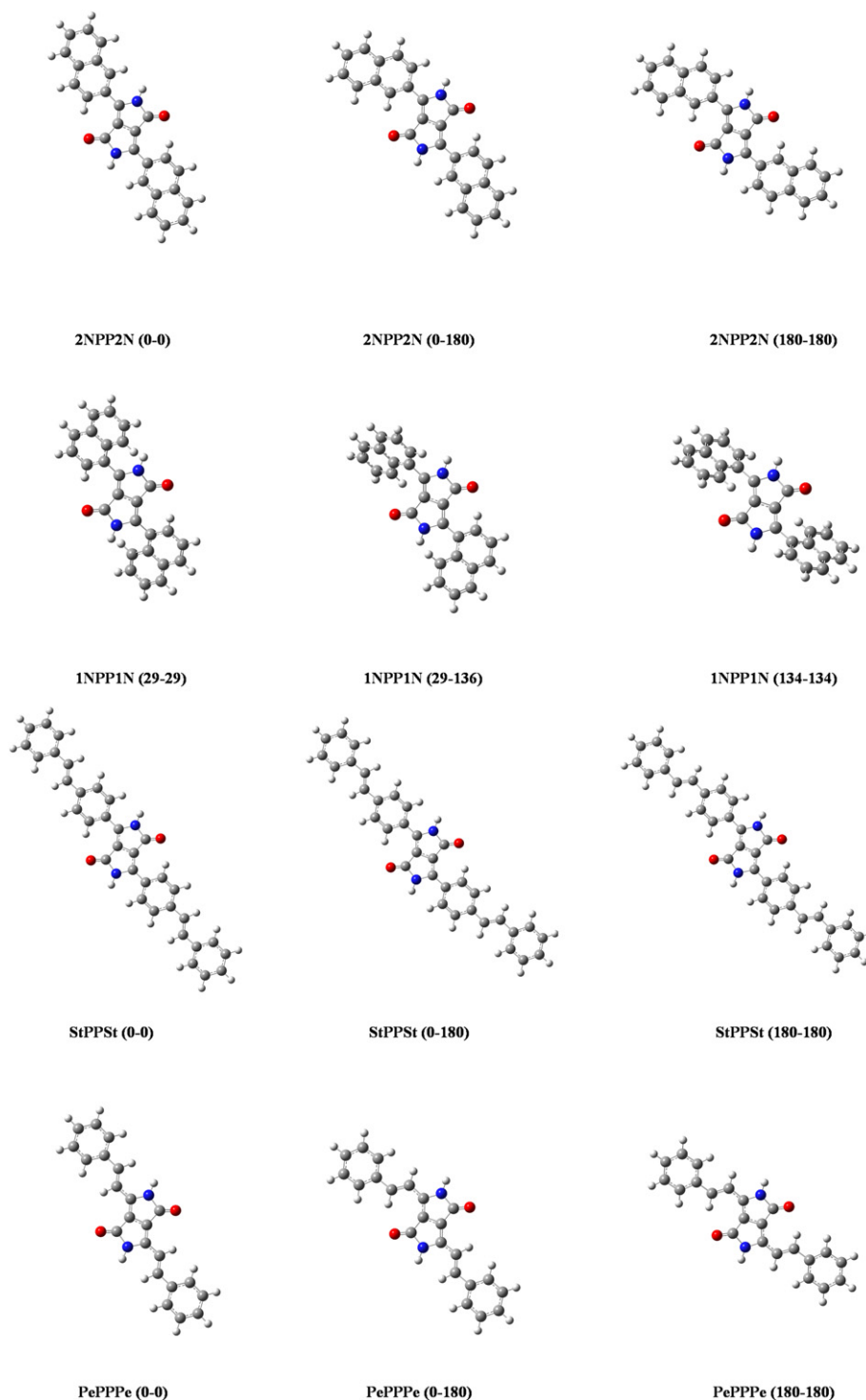


Fig. 1. Rotamers of **2NPP2N**, **1NPP1N**, **StPPSt** and **PePPPe**.

non-bonded to pyrrolinone ring with either N–H or C=O group. Furthermore, each of them can theoretically exist in two rotameric forms differing by a mutual sense of aryl rotations. In summary, 4 (6) minima should exist for **1NPPB** (**1NPP1N**).

Only two of the theoretical four minima were found for **1NPPB**, showing the naphthyl-pyrrolinone dihedral angle 29° (136°) and phenyl-pyrrolinone angle 7° in both cases. Even if the starting geometry favoured the rotamer with opposite sense of phenyl rotation (173–136, 173–29), the geometry converged to the above

mentioned ones (7–136, 7–29). The energy difference is not negligible in this case: the **1NPPB** (7–136) is 1.32 kcal/mol higher in energy than **1NPPB** (7–29), so the steric interaction in an arrangement, where the naphthalene ring non-bonded to pyrrolinone is closer to carbonyl group, is more pronounced.

All six possible rotamers of **1NPP1N** were found as the local minima at this level of calculation. Three rotamers with the same sense of aryl rotations corresponding to  $C_i$  symmetry for (29–29) and (134–134) dihedral angle sets are shown in Fig. 1, too. The

energy difference between the pair of rotamers with opposite sense of aryl rotations is low (less than 1 kcal mol<sup>-1</sup>), preferring C<sub>2</sub> symmetry. The energy difference among three rotamers differing by a mutual orientation of naphthalene with respect to carbonyl group are more pronounced: (29–136) and C<sub>2</sub> (136–136) rotamers are higher in energy with respect to the most stable one C<sub>2</sub> (29–29) for 1.31 kcal mol<sup>-1</sup> and 2.48 kcal mol<sup>-1</sup>, respectively.

Generally, any rotamer of 2-naphthyl derivatives is always more stable than the most stable 1-naphthyl isomer. The differences between the most stable ones are 4.87 kcal mol<sup>-1</sup> between **1NPPB** (7–29) and **2NPPB** (0–180), and 9.64 kcal mol<sup>-1</sup> between **1NPP1N** (C<sub>2</sub> (29–29)) and **2NPP2N** (180–180).

Stilbenyl derivatives (only *trans* arrangement was taken into account) are completely planar by theory, so as the styryl ones (Fig. 1). The former ones evoke the 2-naphthyl DPPs with a marginal differences of the ground state energy between all rotamers, while the latter ones are closer to 1-naphthyl DPPs with indispensable differences among the rotamers' energies (Table 3).

The experimental X-ray structures are available only for **BPPB** [4] and **BiPPBi** [5]. The computed geometry of both compounds well predicts aromatic character of phenyl rings and bond lengths alternation in diketo-pyrrolo-pyrrole moiety. The main difference between computed geometry and that obtained from X-ray diffraction on crystals is in planarity. According to X-ray diffraction the pendant phenyl groups on both compounds are twisted with respect to the heterocycle plane. The dihedral angle is reported to be equal to 7° for **BPPB** [4] and the molecule is of C<sub>i</sub> symmetry in crystal. The dihedral angle phenyl-pyrrolinone is 18–19° for **BiPPBi**, the phenyl–phenyl one is 33° and the molecule is of C<sub>i</sub> symmetry in crystal, because the C<sub>i</sub> symmetry is slightly distorted through a non-planarity (4°) on central dipyrrolinone heterocycle.

We have discussed the non-planarity of further DPP pigments, whose X-ray structures are available, in our previous study [1] and ascribed the non-zero dihedral angles between phenyl and pyrrolinone planes to packing effects in crystal phase. The phenyl–phenyl dihedral angle in biphenyl moiety is less important for a good prediction of spectral behaviour, so the difference about 5° between computed and experimental values is acceptable.

### 3.3. PCM TD DFT vertical excitation energies in DMSO

The vertical excitation energies of the lowest electronic transition recomputed to wavelengths ( $\lambda_{\max}$ ) and oscillator strengths ( $f_{\text{osc}}$ ) of all the compounds computed using PCM TD DFT (B3LYP/6-311 + G(2d,p)) on B3LYP/6-311G(d,p) geometry in dimethylsulfoxide (DMSO) are summarized in Table 3. Table S1 in Supplementary information contains the computed spectral characteristics of four lowest S<sub>0</sub> → S<sub>n</sub> transitions. The lowest excited state is always of S<sub>1</sub>( $\pi\pi^*$ ) character, and the transition S<sub>0</sub> → S<sub>1</sub> is symmetry allowed of HOMO → LUMO type, significantly (always more than 90 nm) separated from the nearest forbidden state (either on carbonyl localized  $n\pi^*$  or HOMO → LUMO + 1 delocalized  $\pi\pi^*$ ).

The difference in  $\lambda_{\max}$  and  $f_{\text{osc}}$  between C<sub>2</sub> and C<sub>i</sub> rotamers of **BiPPBi** is negligible for the first three transitions. Each phenyl substitution brings the same bathochromic shift of S<sub>0</sub> → S<sub>1</sub> transition (19 nm), when going from **BPPB** through **BiPPB** to **BiPPBi**, accompanied by almost linear hyperchromic shift (Table 3). On the other hand the energies of S<sub>0</sub> → S<sub>1</sub> transition of 2-naphthyl derivatives depends on a rotamer type strongly. The increment in predicted  $\lambda_{\max}$  values is about 10 nm per one naphthyl rotation, the most bathochromically shifted rotamers are **2NPP2N** (180–180) and **2NPPB** (0–180). Rather surprisingly, this bathochromic trend among the rotamers is accompanied by the hypochromic one. Bathochromic and hyperchromic shift is also linear when going from **BPPB** through **2NPPB** to **2NPP2N** and the rotamers with

corresponding arrangement of 2-naphthyl substituent with respect to pyrrolinone are taken into account: e.g. the increment in  $\lambda_{\max}$  is 15 nm for an arrangement with dihedral angles equal to 0° and the values of  $f_{\text{osc}}$  are almost the same as for biphenyl set.

The rotamers in stilbenyl set show marginal differences of  $\lambda_{\max}$  values and moderate ones for  $f_{\text{osc}}$ . On the other hand the styryl derivatives resemble the 2-naphthyl set; the dependence of these spectral features on a rotameric arrangement is even more pronounced, including the coupled batho and hypochromic trends among the rotamers. Generally, any increase of a conjugated system of pendant aryls leads to bathochromic shift with respect to parent **BPPB** for planar DPPs. The most efficient is stilbene, followed closely by styryl. The position of biphenyl and 2-naphthyl in this sequence depends on a rotameric form of 2-naphthyl DPPs. The S<sub>0</sub> → S<sub>1</sub> transition energies of unsymmetrical derivatives lie approximately in the middle of the interval between the corresponding values of symmetrical analogues and **BPPB**, oscillator strengths are close to their arithmetic mean.

The excitation energies predicted for 1-naphthyl derivatives are strongly dependent on a degree of non-planarity. The position of  $\lambda_{\max}$  covers a wide range from the values close to the parent **BPPB** for the most distorted rotamers to the values similar as for their planar 2-naphthyl isomers. Rather surprisingly,  $f_{\text{osc}}$  depends on a geometry only moderately, probably because the hyperchromic trend, caused by an increase of conjugated system, is compensated by a hypochromic trend, resulting from a planarity perturbation.

### 3.4. Experimental absorption and fluorescence excitation spectra

All compounds, except **1NPP1N** and **1NPPB**, show very limited solubility even in DMSO at room temperature. The worst soluble compounds are **BiPPBi**, **2NPP2N** and **StPPSt**, all showing the spectral artefacts. The spectrum of **2NPP2N** (and **BiPPBi**, too) shows a long wavelength tailing caused by a light scattering of the unsoluted particles of a pigment. The spectrum of **StPPSt** has furthermore a long wavelength spectral band at 612 nm, that can be probably attributed to dimer or higher aggregate (Fig. 2). Both types of spectral artefacts are not detected in fluorescence excitation spectra of these compounds. Other derivatives are better soluble and a complete agreement between absorption and fluorescence excitation is observed.

The absorption spectra of all compounds except **1NPP1N** and **1NPPB** (Fig. 3) show the spectral shape very similar to parent **BPPB**. Their vibronic structure, well resolved even in DMSO at room temperature, enables the identification of 0–0 vibronic sub-band, that can be compared with the theoretical value. This sub-band

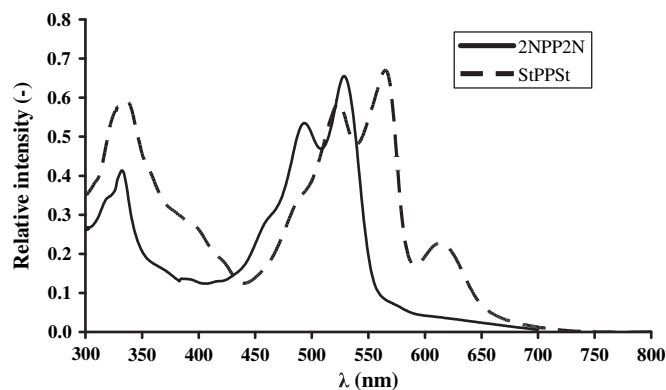


Fig. 2. The room temperature absorption spectra of DMSO solutions of **StPPSt** and **2NPP2N**.

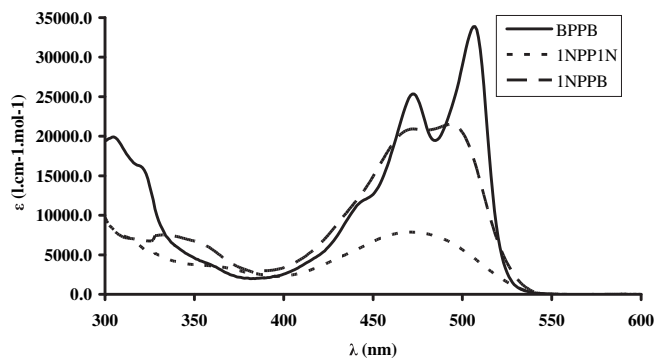


Fig. 3. The room temperature absorption spectra of DMSO solutions of **BPPB**, **1NPP1N** and **1NPPB**.

forms also an absolute spectral maximum. All compounds fluoresce in DMSO, showing approximately a mirror symmetry relation between excitation and emission. The wavelengths of absorption and emission 0–0 vibronic sub-bands are summarized in Table 2. Stokes shift lies between 10 and 20 nm. The vibronic structure is further sharpened in low temperature (77 K) 2-methyl-tetrahydrofuran (MTHF) glass, at which the fluorescence emission and excitation spectra were measured. The typical behaviour is shown in Fig. 4 for **StPPB**. The excitation maxima are shifted bathochromically, as MTHF glass is even more polar environment than DMSO solution [17], and the emission maxima hypsochromically, as the excited state relaxation processes are limited in rigid glass. Finally, Stokes shift is decreased to 2–5 nm (Table 2). **BiPPBi**, **2NPP2N** and **StPPSt** were not sufficiently soluble in MTHF even at concentrations lower than  $10^{-6}$  M to measure their low temperature fluorescence emission and excitation spectra.

1-Naphthyl derivatives show partially (**1NPPB**) or fully (**1NPP1N**) blurred vibronic structure (Fig. 3) in DMSO, as a consequence of non-planarity, so an identification of 0–0 vibronic transition is difficult, especially for **1NPP1N**. Their low temperature fluorescence excitation spectra show quite well resolved vibronic structure for **1NPPB** (Fig. 5) and rather worse resolution for **1NPP1N** (Fig. 6). Evolution of the spectra when going from room to low temperature may be considered as an evidence, that the absolute spectral maximum corresponds to 0–0 vibronic transition for **1NPPB** and probably to 0–1 transition for **1NPP1N**.

If we do not consider both non-planar 1-naphthyl DPPs for this moment, we can see several clear trends. Larger conjugated system of an aryl substituent causes a bathochromic shift;  $\lambda_{\text{abs}}$  of unsymmetrical derivative is exactly an arithmetic mean of parent **BPPB** and

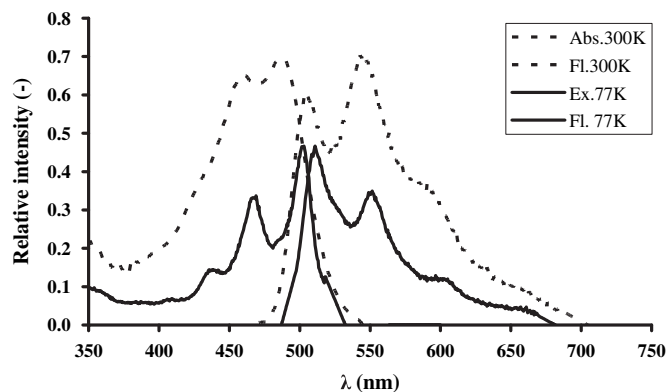


Fig. 5. The room temperature absorption and fluorescence emission and low temperature fluorescence emission and excitation spectra of **1NPPB** in MTHF.

corresponding symmetrical derivative as predicted by theory. When going from **BPPB** to all three unsymmetrical derivatives, a hyperchromic shift is observed, also in a qualitative agreement with computational results. But molar absorptivities of all three unsymmetrical derivatives are lower than those ones of corresponding symmetrical ones, on the contrary to the theoretical results, predicting approximately linear increase. The main reason for this discrepancy is an extremal insolubility of symmetrical pigments, making impossible a correct estimation of  $\epsilon_{\text{max}}$ . The difference in  $\epsilon_{\text{max}}$  values between **BPPB** and **BiPPB** is  $5900 \text{ l mol}^{-1} \text{ cm}^{-1}$ , so the similar value should be expected according to theoretical predictions between **BiPPB** and **BiPPBi**. Thus  $\epsilon_{\text{max}}$  value of **BiPPBi**, extrapolated from better soluble **BPPB** and **BiPPB**, is  $46\,000 \text{ l mol}^{-1} \text{ cm}^{-1}$ , while the experimental one is  $17\,300 \text{ l mol}^{-1} \text{ cm}^{-1}$ . The value of **2NPP2N** of  $\epsilon_{\text{max}}$  is also lower ( $30\,400 \text{ l mol}^{-1} \text{ cm}^{-1}$ ) than the one derived by extrapolation from **BPPB** and **2NPPB** ( $40\,200 \text{ l mol}^{-1} \text{ cm}^{-1}$ ), although the difference is not so dramatic as for biphenyl set. The same type of inconsistency between the value ( $54\,400 \text{ l mol}^{-1} \text{ cm}^{-1}$ ) extrapolated from **BPPB** and **StPPB** and experimental ( $33\,600 \text{ l mol}^{-1} \text{ cm}^{-1}$ ) one for **StPPSt** is observed, too, from the same reasons.

There is quite a good agreement between computed and experimental maxima for **BPPB**, **BiPPB** and **BiPPBi**, for which either there is only one possible geometry or both rotamers give the same theoretical  $\lambda_{\text{max}}$ . The experimental maxima are always at rather longer wavelengths, but the differences are acceptable (11 nm, 7 nm and 4 nm). The situation seems to be similar to that one described in Ref. [1]: the *para* substituted derivatives of **BPPB** are computed rather better than the parent chromophore itself.

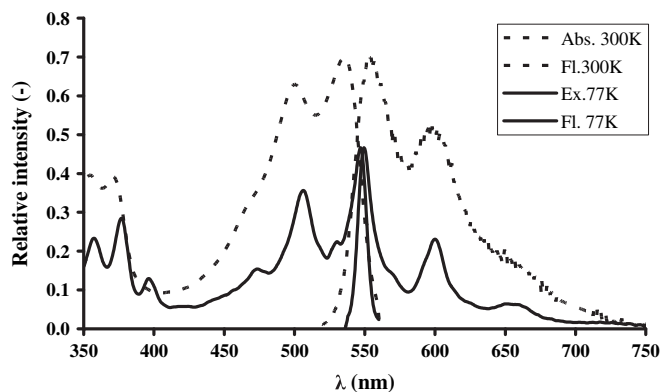


Fig. 4. The room temperature absorption and fluorescence (DMSO) and low temperature (MTHF) fluorescence emission and excitation spectra of **StPPB**.

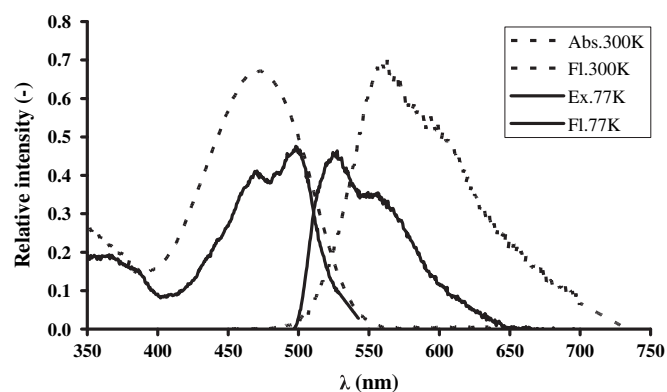


Fig. 6. The room temperature absorption and fluorescence emission and low temperature fluorescence emission and excitation spectra of **1NPP1N** in MTHF.



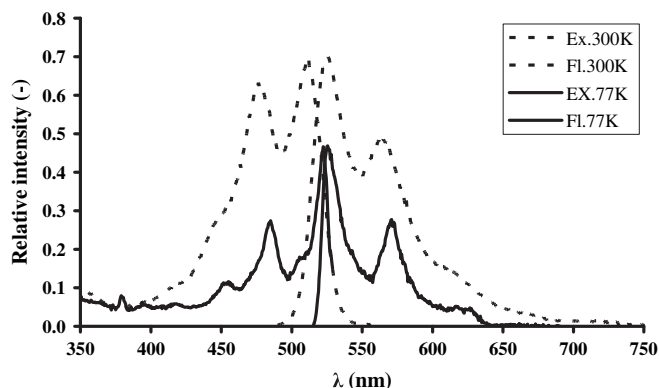


Fig. 7. The room and low temperature fluorescence emission and excitation spectra of **2NPPB** in MTHF.

No dependence of the fluorescence emission spectrum on the excitation wavelength (and opposite) was observed for any sample, either at room or low temperature. As the difference in absorption maxima of rotamers of 2-naphthyl derivatives should be about 10 nm, a similar value as experimentally obtained for rotamers of 2-naphthyl-ethylenes, we can conclude, that only one rotamer of **2NPPB** and **2NPP2N** is present in solution [18], although their ground state energy is almost the same. Furthermore, a mixture of spectrally shifted rotamers could hardly produce the spectra with such sharp vibronic structure as shown in Fig. 7. Thus the question arises, whether the rotamer present in solution can be estimated by a comparison of the experimental and theoretical  $\lambda_{\text{max}}$ . The experimental values are closer for **2NPPB** (0–0) rotamer and lie between **2NPP2N** (0–0) and **2NPP2N** (0–180) rotamers. Thus, if we suppose, that the same orientation of naphthalene ring is preferred in both compounds, the rotamers characterized by dihedral angle equal to 0 (Fig. 1) can be concluded as more probable. This assignment is also consistent with a comparison of **2NPPB** (0–0) with **BiPPB**: the difference in  $\lambda_{\text{max}}$  is 4 (3) nm by theory (experiment) and  $\epsilon_{\text{max}}$  are very close as predicted.

On the contrary to 2-naphthyl and biphenyl derivatives the experimental absorption maxima of stilbenyl ones are considerably blue shifted with respect to the theoretical values. Furthermore, molar absorptivity of **StPPB** is only a bit higher than for **BiPPB**, although the theoretical prediction supposes a higher value of  $\epsilon_{\text{max}}$ . We consider two sources of this discrepancy. First, *trans*-stilbene, although planar in crystal [19] and by high level quantum chemical calculations [20], is often considered as non-planar in solution with both phenyls partially rotated out-of-plane [21]. Such rotation could cause a considerable hypsochromic and hypochromic shift, if present in **StPPB** and **StPPSt**. Second, both stilbenyl derivatives show the longest conjugated chain in one direction, that can be a problem for TD DFT method, because of its known incorrect asymptotic behaviour with respect to the long distance between charges [22]. Both these effect can be less significant in styryl derivatives **PePPB** and **PePPPe**, so it is possible, that they could be experimentally bathochromically shifted with respect to stilbenyl analogues, although the theory predicts the opposite relation. Thus it is desirable to find a synthetic alternative for them [6].

The most controversial results were obtained for non-planar well soluble 1-naphthyl derivatives. They show significantly higher Stokes shift in DMSO, dramatically decreased in MTHF glass, mainly as a consequence of limited ability of excited state geometrical relaxation in rigid environment. The experimental values of  $\epsilon_{\text{max}}$  are significantly decreased with respect to parent chromophore or to 2-naphthyl isomers as qualitatively expected for the lost planarity, but not quantitatively predicted by TD DFT. Furthermore,

the value extrapolated from **BPPB** and **1NPPB** ( $8800 \text{ l mol}^{-1} \text{ cm}^{-1}$ ) is close to the experimental one ( $7900 \text{ l mol}^{-1} \text{ cm}^{-1}$ ) for **1NPP1N**, that is only qualitatively in accordance with theory and only for the most distorted rotamer set, e.g. **BPPB**  $\rightarrow$  **1NPPB** (7–136)  $\rightarrow$  **1NPP1N** ( $C_i$ , 134–134). Even if we take into account, that the absorption maximum of **1NPP1N** corresponds to 0–1 vibronic transition, experimental  $\lambda_{\text{max}}$  of both 1-naphthyl derivatives show a hypsochromic shift with respect to parent **BPPB** on the contrary to the theoretical predictions for any rotamer. Simply said, the computations underestimate the excitation energies and overestimate the probability of spectral transitions. We do think, that the explanation of this discrepancy comes from the underestimation of dihedral angles by DFT calculations of the ground state geometry. The synthesis of further non-planar symmetrical and unsymmetrical till unknown DPPs, with N-heteroaryles coming from 4-cyano-quinoline and 1-cyano-isoquinoline, is now in progress. Thus, we return to the detailed discussion of 1-naphthyl DPPs with similar steric hindrance after collecting more experimental data from their N-heteroanalogues.

#### 4. Conclusions

The effect of a size of a conjugation system of aryl substituents on the absorption spectra of diketo-pyrrolo-pyrroles was studied. Two new unsymmetrical derivatives were synthesized in order to complete the investigated set. PCM TD DFT calculations predict a linear increase of both  $\lambda_{\text{max}}$  and  $\epsilon_{\text{max}}$  with a substitution of each phenyl in parent **BPPB** by larger aryl for planar derivatives. Qualitatively, the experimental bathochromic shifts of 0–0 vibronic subbands are in exact agreement with theory, while the hyperchromic shifts are affected by extremely low solubility of planar symmetrical derivatives. Quantitatively, the theory only slightly overestimates the excitation energies in this case. The deviations from this ideal behaviour were observed for non-planar derivatives (aryl = stilbenyl or 1-naphthyl), for which the dihedral angles describing the aryl out-of-plane torsions are probably underestimated by DFT.

#### Acknowledgments

Authors acknowledge the support of the grant project No. 2A-1TP1/041 sponsored by the Ministry of Trade and Industry of the Czech Republic.

#### Appendix. Supplementary information

Supplementary data associated with this article can be found, in the online version, at doi:10.1016/j.dyepig.2009.09.014.

#### References

- [1] Luňák Jr S, Vyňuchal J, Vala M, Havel L, Hrdina R. The syntheses, absorption and fluorescence of polar diketo-pyrrolo-pyrroles. *Dyes Pigments* 2009; 82:102–8.
- [2] Iqbal A, Cassar L. EP 98808 (Ciba-Geigy, 1982).
- [3] Herbst M, Hunger K. Industrial organic pigments. Weinheim: VCH; 1993.
- [4] Mizuguchi J, Rihs G. Electronic spectra of 1,4-diketo-3,6-diphenyl-pyrrolo-[3,4-c]-pyrrole in the solid-state. *Ber Bunsenges Phys Chem* 1992;96(4): 597–606.
- [5] Mizuguchi J, Miyazaki T. Crystal structure of 3,6-bis(4-biphenyl)pyrrolo[3,4-c]pyrrole-1,4-dione,  $C_{30}H_{20}N_2O_2$ . *Z Kristallogr - New Cryst Struct* 2002;217:43–4.
- [6] Morton CJH, Gilmour R, Smith DM, Lightfoot P, Slawin AMZ, MacLean EJ. Synthetic studies related to diketopyrrolopyrrole (DPP) pigments. Part 1: the search for alkenyl DPPs. Unsaturated nitriles in standard DPP syntheses: a novel cyclopenta[c]pyrrolone chromophore. *Tetrahedron* 2002;58:5547–65.
- [7] Iqbal A, Kirchmayr R, Pfenninger J, Rochat AC, Wallquist O. The synthesis and properties of 1,4-diketo-pyrrolo[3,4-c]pyrroles. *Bull Soc Chim Belges* 1988;97(8–9):615–43.

- [8] Adachi A, Nakamura S. Absorption spectrum shift in the solid state. A MO study of pyrrolopyrrole pigment. *J Phys Chem* 1994;98:1796–801.
- [9] Wallquist O. In: Smith HM, editor. High performance pigments. Weinheim: Wiley-VCH; 2002. p. 159–84.
- [10] Vala M, Weiter M, Vyňuchal J, Toman P, Luňák Jr S. Comparative studies of diphenyl-diketo-pyrrolopyrrole derivatives for electroluminescence applications. *J Fluoresc* 2008;18(6):1181–6.
- [11] Vyňuchal J, Luňák Jr S, Hatlapatková A, Hrdina R, Lyčka A, Havel L, et al. The synthesis, absorption, fluorescence and photoisomerisation of 2-aryl-4-aryl-methylidene-pyrroline-5-ones. *Dyes Pigments* 2008;77(2):266–76.
- [12] Wang L, Li H, Li P. Task-specific ionic liquid as base, ligand and reaction medium for the palladium-catalyzed Heck reaction. *Tetrahedron* 2009;65(1):364–8.
- [13] Becke AD. Density-functional thermochemistry. III. The role of exact exchange. *J Chem Phys* 1993;98:5648–52.
- [14] Jacquemin D, Perpète EA, Ciofini I, Adamo C. Accurate simulation of optical properties in dyes. *Acc Chem Res* 2009;42:326–34.
- [15] Tomasi J, Mennucci B, Cammi R. Quantum mechanical continuum solvation models. *Chem Rev* 2005;105:2999–3094.
- [16] Gaussian 03 W, Frisch MJ, Trucks GW, Schlegel HB, Scuseria GE, Robb MA, Cheeseman JR, Montgomery Jr JA, Vreven T, Kudin KN, Burant JC, Millam JM, Iyengar SS, Tomasi J, Barone V, Mennucci B, Cossi M, Scalmani G, Rega N, Petersson GA, Nakatsuji H, Hada M, Ehara M, Toyota K, Fukuda R, Hasegawa J, Ishida M, Nakajima T, Honda Y, Kitao O, Nakai H, Klene M, Li X, Knox JE, Hratchian HP, Cross JB, Bakken V, Adamo C, Jaramillo J, Gomperts R, Stratmann RE, Yazyev O, Austin AJ, Cammi R, Pomelli C, Ochterski JW, Ayala PY, Morokuma K, Voth GA, Salvador P, Dannenberg JJ, Zakrzewski VG, Dapprich S, Daniels AD, Strain MC, Farkas O, Malick DK, Rabuck AD, Raghavachari K, Foresman JB, Ortiz JV, Cui Q, Baboul AG, Clifford S, Cioslowski J, Stefanov BB, Liu G, Liashenko A, Piskorz P, Komaromi I, Martin RL, Fox DJ, Keith T, Al-Laham MA, Peng CY, Nanayakkara A, Challacombe M, Gill PMW, Johnson B, Chen W, Wong MW, Gonzalez C, Pople JA. Wallingford, CT: Gaussian, Inc.; 2004.
- [17] Zoon PD, Brouwer AM. A push–pull aromatic chromophore with a touch of merocyanine. *Photochem Photobiol Sci* 2009;8:345–53.
- [18] Castel N, Fischer E, Bartocci G, Masetti F, Mazzucato U. Viscosity-induced emission anomalies in 1,2-diarylethenes and distyryl-benzenes and -naphthalenes. *J Chem Soc Perkin Trans II* 1985, 1969–75.
- [19] Bouwstra JA, Schouten A, Kroon J. Structural studies of the system trans-azobenzene/trans-stilbene. II. A reinvestigation of the disorder in the crystal structure of trans-stilbene, C<sub>14</sub>H<sub>12</sub>. *Acta Crystallogr C* 1984;40:428–31.
- [20] Watanabe H, Okamoto Y, Furuya K, Sakamoto A, Tasumi M. Vibrational analysis of trans-stilbenes in the ground and excited singlet electronic states revisited. *J Phys Chem A* 2002;106:3318–24.
- [21] Catalán J. On the nonplanarity of trans-stilbene. *Chem Phys Lett* 2006;421:134–7.
- [22] Dreuw A, Head-Gordon M. Single-reference ab initio methods for the calculation of excited states of large molecules. *Chem Rev* 2005;102(11):4009–37.